The Dilated Cardiomyopathy G159D Mutation in Cardiac Troponin C Weakens the Anchoring Interaction with Troponin I[†]

Olga K. Baryshnikova,[‡] Ian M. Robertson,[‡] Pascal Mercier, and Brian D. Sykes*

Department of Biochemistry, University of Alberta, Edmonton, Alberta, Canada T6G 2H7

Received June 22, 2008; Revised Manuscript Received August 18, 2008

ABSTRACT: NMR spectroscopy has been employed to elucidate the molecular consequences of the DCM G159D mutation on the structure and dynamics of troponin C, and its interaction with troponin I (TnI). Since the molecular effects of human mutations are often subtle, all NMR experiments were conducted as direct side-by-side comparisons of the wild-type C-domain of troponin C (cCTnC) and the mutant protein, G159D. With the mutation, the affinity toward the anchoring region of cTnI ($cTnI_{34-71}$) was reduced ($K_D = 3.0 \pm 0.6\ \mu M$) compared to that of the wild type ($K_D < 1\ \mu M$). Overall, the structure and dynamics of the G159D·$cTnI_{34-71}$ complex were very similar to those of the cCTnC·$cTnI_{34-71}$ complex. There were, however, significant changes in the ^1H, ^{13}C, and ^{15}N NMR chemical shifts, especially for the residues in direct contact with $cTnI_{34-71}$, and the changes in NOE connectivity patterns between the G159D·$cTnI_{34-71}$ and cCTnC·$cTnI_{34-71}$ complexes. Thus, the most parsimonious hypothesis is that the development of disease results from the poor anchoring of cTnI to cCTnC, with the resulting increase in the level of acto-myosin inhibition in agreement with physiological data. Another possibility is that long-range electrostatic interactions affect the binding of the inhibitory and switch regions of cTnI ($cTnI_{128-147}$ and $cTnI_{147-163}$) and/or the cardiac specific N-terminus of cTnI ($cTnI_{1-29}$) to the N-domain of cTnC. These important interactions are all spatially close in the X-ray structure of the cardiac TnC core.

Calcium regulation of contraction in cardiac muscle is a fine-tuned process that depends on the reliable function of its protein parts. The presence of mutations in contractile proteins can cause the development of cardiac disorders. Indeed, as revealed by genetic analysis, a large number of mutations in β-myosin, α-tropomyosin, cardiac troponin I (cTnI),[1] and cardiac troponin T (cTnT) cause various forms of cardiomyopathy (*1, 2*). Cardiac troponin C (cTnC), the protein directly responsible for Ca^{2+} sensitivity of the thin filament, is highly conserved among mammals and was thought to have fewer mutations until recently (*3*−*5*).

Troponin C is a dumbbell-shaped molecule with its structural domain (cCTnC) linked to its regulatory domain (cNTnC) through a stretch of 11 residues. During the contracting−relaxing cycle, cCTnC remains saturated with Ca^{2+} due to its high Ca^{2+} affinity. This domain is thought to be bound at all times to the anchoring region of cTnI (approximately residues 34−71), which tethers cTnC to the thin filament. The Ca^{2+} binding site of cNTnC is occupied only when the concentration of Ca^{2+} is relatively high. This happens upon the release of Ca^{2+} from the sarcoplasmic reticulum resulting from muscle stimulation. When Ca^{2+} binds, cNTnC binds to the switch region of cTnI (approximately residues 147−163), which pulls the inhibitory region of cTnI (approximately residues 128−147) away from its binding site on actin, leading to the movement of tropomyosin and the exposure of myosin binding sites on actin, allowing the contraction (for reviews, see refs *6* and *7*).

Two mutations found in cNTnC, L29Q and E59D/D75Y, were linked to hypertrophic cardiomyopathy (FHC) and dilated cardiomyopathy (DCM), respectively (*3, 8*). As demonstrated in physiological experiments, L29Q resulted in a slight increase of the Ca^{2+} sensitivity of force development (*9*). L29Q also abolished the impact of phosphorylation on the activity of ATPase, the sliding velocity of the thin filament (*10*), and the kinetics of binding of Ca^{2+} to the troponin complex (*11*). The presence of the E59D/D75Y double mutation resulted in a weakened ability to activate myosin ATPase (*12*) and a decreased Ca^{2+} sensitivity of force development (*8*). In structural studies (*13*), mutations L29Q and E59D/D75Y affected the interplay between the cardiac specific N-terminus of cTnI (approximately residues 1−29) and the switch region of cTnI (approximately residues 147−163), the binding of which is crucial for the transfer of the Ca^{2+} signal through cTnC and further along the thin filament. In L29Q, the affinity for $cTnI_{147-163}$ was not affected by the $cTnI_{1-29}$ phosphorylation and in the presence of $cTnI_{1-29}$ was stronger than the wild-type value. In E59D/D75Y, the affinity for $cTnI_{147-163}$ was weakened in the presence of $cTnI_{1-29}$. Thus, the physiological consequences of the L29Q and E59D/D75Y mutations and disease devel-

[†] This work was supported by an Alberta Heritage Foundation for Medical Research scholarship (O.K.B.) and a grant from the Canadian Institutes for Health Research.

* To whom correspondence should be addressed. Phone: (780) 492-5460. Fax: (780) 492-0886. E-mail: brian.sykes@ualberta.ca.

[‡] These authors contributed equally to this work.

[1] Abbreviations: cCTnC, C-domain of cardiac troponin C; cNTnC, N-domain of cardiac troponin C; DCM, dilated cardiomyopathy; FHC, familial hypertrophic cardiomyopathy; G159D, G159D mutant of the C-domain of cardiac troponin C; NOE, nuclear Overhauser effect; cTnI, cardiac troponin I; DSS, 2,2-dimethyl-2-silapentane-5-sulfonate sodium salt.

10.1021/bi801165c CCC: $40.75
Published on Web 09/20/2008

opment can be related to the impaired thermodynamics of the interactions of cNTnC with its binding partners, $cTnI_{1-29}$ and $cTnI_{147-163}$.

Another mutation, G159D, linked to DCM, was found in cCTnC (*4*). In reconstituted rat (*14*) and rabbit (*15*) cardiac trabeculae, the presence of G159D did not significantly alter myofilament Ca^{2+} sensitivity. However, the presence of the G159D mutation in guinea pig trabeculae resulted in reduced Ca^{2+} sensitivity (*16*). Available physiological data on G159D reported the reduced activity of ATPase (*16*); however, the Ca^{2+} sensitivity of ATPase was not affected (*14*). It might be difficult to interpret physiological results at the molecular level, especially since Ca^{2+} sensitivity is a complex function of many consequential events, such as the binding of Ca^{2+}, the binding of $cTnI_{147-163}$, and the attachment of cross-bridges, and since the reproducibility of the results was thought to be dependent on muscle fiber type (*15*). We have attempted to address this question using the G159D mutant of cCTnC and the cTnI peptide ($cTnI_{34-71}$), so that the interactions between troponin parts can be unambiguously traced. The knowledge of these interactions can be compiled afterward into the overall picture that assists in the interpretation of the physiological data.

There are several functions attributed to cCTnC, which could be affected by the presence of G159D. First, in its Ca^{2+}-bound form, cCTnC binds to the anchoring region of cTnI (approximately residues 34−71) and tethers the entire troponin complex to the thin filament. Second, cCTnC binds the inhibitory region of cTnI (approximately residues 128−147), the location of which has not been visualized in available crystal structures (*17*) and is suspected to be driven by electrostatics (*18, 19*). The binding of $cTnI_{128-147}$ occurs without replacement of $cTnI_{34-71}$ and is hypothesized to be localized next to the highly charged E−D linker connecting two domains of cTnC. Third, cCTnC was also shown to interact with cTnT (*20*). Fourth, G159D might affect the interaction with the cardiac specific N-terminus of cTnI (approximately residues 1−34), which was suspected in experiments with skinned rat trabeculae (*14*) and with the reconstituted troponin complex (*11*). In the crystal structure, Gly^{159} is located at the very end of the H-helix, 5 Å from Leu^{47} of the anchoring region of cTnI (approximately residues 34−71) (*17*). This suggests that the presence of the mutation might first of all affect the interaction with $cTnI_{34-71}$, which has not been addressed previously. Using NMR spectroscopy, we have determined the affinity of G159D for $cTnI_{34-71}$ and examined the consequences of this mutation on the structure and dynamics of the G159D·$cTnI_{34-71}$ complex. On the basis of NOE connectivity patterns, NMR chemical shift changes, dynamics, and three-dimensional structures, we conclude that compared to cCTnC, G159D binds to $cTnI_{34-71}$ in a similar fashion, albeit with a lower affinity. This interaction is a key function of cCTnC and, when impaired, can perturb the function of the entire Tn complex and lead to severe physiological consequences, such as the development of cardiomyopathy.

EXPERIMENTAL PROCEDURES

Protein Expression and Purification. The DNA encoding cCTnC (residues 91−161) was subcloned previously into the pET-3a expression vector in a manner similar to that of Pearlstone et al. (*21*). Using cCTnC as a template, the G159D mutation was engineered using a site-directed mutagenesis kit (QuikChange purchased from Stratagene). *Escherichia coli* strain BL21(DE3)pLysS was transformed with the expression vector and incubated at 37 °C to an OD_{600} of 0.6−0.9. Cell cultures were induced with IPTG and harvested after being incubated for 3 h. Uniformly ^{15}N-labeled or ^{13}C- and ^{15}N-labeled cCTnC and G159D were expressed in a minimal medium enriched with $(^{15}NH_4)_2SO_4$ or $(^{15}NH_4)_2SO_4$ and [^{13}C]glucose (*22*). The cell pellet was lysed using a French press and applied to a DEAE column [50 mM Tris and 0.1 M NaCl (pH 8.0)]. Proteins were further purified using a Superdex-75 size exclusion column [50 mM Tris and 0.15 M NaCl (pH 8.0)], desalted using a Sephadex G25 column (10 mM NH_4HCO_3), and lyophilized. Molecular masses for unlabeled proteins, cCTnC and G159D, as determined by MALDI mass spectrometry were equal to the expected values. The amino acid composition was confirmed independently by amino acid analysis.

$cTnI_{34-71}$ Titration of cCTnC and G159D Monitored by Two-Dimensional (2D) $^1H-^{15}N$ HSQC NMR Spectroscopy. The peptide $cTnI_{34-71}$ (acetyl-AKKKSKISASRKLQLK-TLLLQIAKQELEREAEERRGEK-amide) was synthesized using a standard methodology for a typical TnI peptide (*23*). The sequence was confirmed by amino acid analysis, and the mass was verified by electrospray mass spectrometry. During titration, the peptide was added in the form of powder to the 500 μL solution of 0.57 mM cCTnC and 0.56 mM G159D. The buffer consisted of 100 mM KCl, 10 mM imidazole, 2 mM $CaCl_2$, 5 mM NaN_3, and 0.2 mM DSS in a 90% H_2O/10% D_2O mixture. The pH was adjusted to 6.7 ± 0.05 at every titration point. Concentrations of proteins and peptides were determined by weight and confirmed by amino acid analysis. Since the reaction proceeds within the slow exchange limits for both cCTnC and G159D, the chemical shifts for two species (cCTnC or G159D alone and in complex with $cTnI_{34-71}$) were observed during titrations. The decreasing intensities of individual amide resonances of uncomplexed cCTnC or G159D were used to calculate K_D. The $cTnI_{34-71}$-induced decrease in amide intensities was averaged for all monitored amides and plotted as a function of $[cTnI_{34-71}]_{total}/[cCTnC]_{total}$ or $[cTnI_{34-71}]_{total}/[G159D]_{total}$. The normalized curve for all monitored amides was fit for both titrations to the equation

$$\text{troponin C} + \text{troponin I} \leftrightarrow \text{troponin C}-\text{troponin I}$$

The dissociation constants measured were in the micromolar range, and since the concentrations of G159D and cCTnC were in the millimolar range, precise comparison of the data was difficult. Therefore, the titration of $cTnI_{34-71}$ was repeated at a much lower G159D concentration. Samples of 42 μM unlabeled G159D and 2 mM unlabeled $cTnI_{34-71}$ were prepared under the buffer conditions summarized above. The titration was performed until a $cTnI_{34-71}$:G159D ratio of ~3:1 was reached. One-dimensional (1D) ^1H NMR spectra of G159D were acquired at each titration point. Isolated peaks in the 1D ^1H spectrum were monitored throughout the titration, and changes in peak intensities as a function of $cTnI_{34-71}$ were used to calculate the K_D. The data were averaged, normalized, and fit using the curve fitting program xcrvfit, version 4.0.12 (http://www.bionmr.ualberta.ca/bds/software/xcrvfit).

Table 1: NMR Relaxation Parameters T_1, T_2, and τ_m Determined for G159D and cCTnC Alone and in Complexes with $cTnI_{34-71}$

	average of per residue T_1 (ms)	average of per residue T_2 (ms)	overall correlation time, τ_m (ns)	theoretical estimate for correlation time, τ_m[a] (ns)
G159D	356 ± 47	193 ± 31	3.3	4.2
G159D·$cTnI_{34-71}$	436 ± 46	112 ± 9	6.6	6.4
cCTnC	348 ± 42	185 ± 25	3.4	4.2
cCTnC·$cTnI_{34-71}$	438 ± 53	109 ± 13	6.5	6.4

[a] The theoretical estimate for correlation time τ_m is equal to half of the molecular mass in kilodaltons.

^{15}N Backbone Amide NMR Relaxation Data. Relaxation data were acquired at 30 °C on a Varian Inova 500 MHz spectrometer during ^{15}N T_1, ^{15}N T_2, and $^1H-^{15}N$ NOE experiments (Biopack, Varian Associates) for 500 μL samples containing 0.57 mM cCTnC or 0.56 mM G159D and 1.2 mM $cTnI_{34-71}$. T_1 values were acquired using relaxation delays of 10, 50, 100, 200, 300, and 400 ms, and T_2 values were acquired using relaxation delays of 10, 30, 50, 70, 90, and 110 ms. Delays between transients in ^{15}N T_2 and ^{15}N T_1 experiments were set to 3 s. $^1H-^{15}N$ NOE experiments were performed using delays of 5 s for spectra recorded without proton saturation and delays of 2 s for spectra recorded with proton saturation. Proton saturation was set to 3 s, so that the total time between transients was equal to 5 s. Relaxation parameters, T_1, T_2, and NOE, were extracted using the rate analysis module built in NMRView (*24*) and analyzed using Mathematica scripts provided by L. Spyracopuolos (www.bionmr.ualberta.ca/~lspy/) (*25*). The overall rotational tumbling time, τ_m, was averaged from the per residue fitting of relaxation data to the Lipari−Szabo $S^2-\tau_m-\tau_f$ model (*26*). Relaxation data for residues with significant internal motions, as judged by a NOE of <0.65, and data for residues with possible slow motions, as judged by a significantly decreased T_2, were excluded in this method of τ_m calculation.

Assignment and Structure Calculation for cCTnC·$cTnI_{34-71}$ and G159D·$cTnI_{34-71}$ Complexes. Samples used for NMR data acquisition contained ~0.5 mM G159D or cCTnC and ~1.2 mM $cTnI_{34-71}$ in a buffer that consisted of 100 mM KCl, 10 mM imidazole, 2 mM $CaCl_2$, 5 mM NaN_3, and 0.2 mM DSS in a 90% H_2O/10% D_2O mixture. The buffer used for data acquisition in D_2O contained 100 mM KCl, 0.5 mM imidazole, 9.5 mM deuterated imidazole, 2 mM $CaCl_2$, 5 mM NaN_3, and 0.2 mM DSS. NMR spectra were acquired at 30 °C on a Varian INOVA 500, Unity 600, or INOVA 800 spectrometer equipped with 5 mm triple resonance probes and z axis pulsed field gradients (Table 3). NMR data were processed using NMRPipe (*27*) and analyzed with NMRView (*24*). The backbone resonances for cCTnC and G159D in the [^{13}C,^{15}N]cCTnC·$cTnI_{34-71}$ and [^{13}C,^{15}N]G159D·$cTnI_{34-71}$ complexes were assigned using SmartNotebook version 5.1.3 (*28*). Side chain assignment was carried out using HCCH-TOCSY, HCCONH, CCONH, HNHA, HNHB, and ^{15}N TOCSY HSQC. The majority of side chain resonances were unambiguously assigned. Resonances for aromatic residues were assigned using 2D homonuclear DQF-COSY and NOESY experiments in D_2O. Resonances for the $cTnI_{34-71}$ peptide were not sufficiently dispersed in 2D ^{13}C/^{15}N-filtered TOCSY and NOESY experiments to allow for the assignment of many residues except for amide protons, HN, for residues 41−64, Hα protons for residues 41−59, Hβ protons for residues 41−43, 50, 53, and 56, and Hδ/γ protons for residues 46−53, 55, and 58−60.

Table 2: Statistics for 20 NMR Structures of G159D and cCTnC in Complex with $cTnI_{34-71}$[a]

	G159D	cCTnC
no. of NOE restraints	1075	957
short-range ($\|i-j\|=1$)	624	561
medium-range ($1<\|i-j\|<5$)	231	215
long-range ($\|i-j\|\geq 5$)	220	181
no. of Ca^{2+} binding restraints	16	16
no. of dihedral restraints (ϕ/ψ)[b]	84	86
NOE violations		
>0.5 Å	0.15 ± 0.37	0.0 ± 0.0
>0.3 Å	0.25 ± 0.55	1.8 ± 1.20
>0.1 Å	6.3 ± 1.95	10.45 ± 2.28
dihedral violations (deg)	0.0 ± 0.0	0.0 ± 0.0
Ramachadran plot statistics[c]		
ϕ/ψ in most favorable regions (%)	93 ± 4	92 ± 4
ϕ/ψ in additionally allowed regions (%)	7 ± 3	7 ± 3
ϕ/ψ in generously allowed regions (%)	0 ± 1	1 ± 1
ϕ/ψ in disallowed regions (%)	0 ± 1	1 ± 1
pairwise rmsd (Å)[d]		
before water refinement	0.71 ± 0.13	0.59 ± 0.12
after water refinement	1.29 ± 0.28	1.31 ± 0.24
WHATCHECK structure Z score after water refinement		
second-generation packing quality	−0.9 ± 0.4	−0.9 ± 0.3
Ramachandran plot appearance	0.9 ± 0.7	1.8 ± 0.8

[a] Structures were calculated using CYANA (*29*), refined using XPLOR-NIH (*32, 33*), and analyzed using PROCHECK (*34*) and WHATCHECK (*35*). [b] Predicted from chemical shifts using TALOS. [c] PROCHECK was used over all the residues (90−161). [d] Main chain nuclei over residues 95−155.

Structure calculations were performed with CYANA (*29*) using the "noeassign" automatic assignment procedure (*30*) and distance restraints from ^{13}C NOESY HSQC and ^{15}N NOESY HSQC experiments. Unambiguous restraints were assigned manually and were forced to keep their assignments during the first four runs of CYANA calculations, after which they were open for automatic assignment by CYANA. Distance restraints were calibrated with the CYANA standard procedure using upper limits of 6 Å. TALOS dihedral restraints for helical regions for G159D and cCTnC (*31*) and Ca^{2+} restraints for Ca^{2+} binding loops were obtained from X-ray crystallographic data and added into the calculation (Table 2). TALOS restraints did not affect the overall fold of the structures (data not shown). In the final structure calculations of G159D, however, the TALOS restraints were truncated up to residue 151. This was done to avoid artifactual secondary structure fabrication from TALOS, since it uses only chemical shift homology from other proteins to predict backbone angles. CYANA was used to calculate 50 structures, of which the 20 conformers with the lowest target function were refined in explicit solvent by XPLOR-NIH (*32, 33*) with a water box edge length of 18.8 Å. The final ensembles were averaged and refined using the same water refinement protocol used previously and are the structures discussed here and deposited in the Protein Data Bank. Structures were validated using PROCHECK (*34*) and WHATCHECK (*35*).

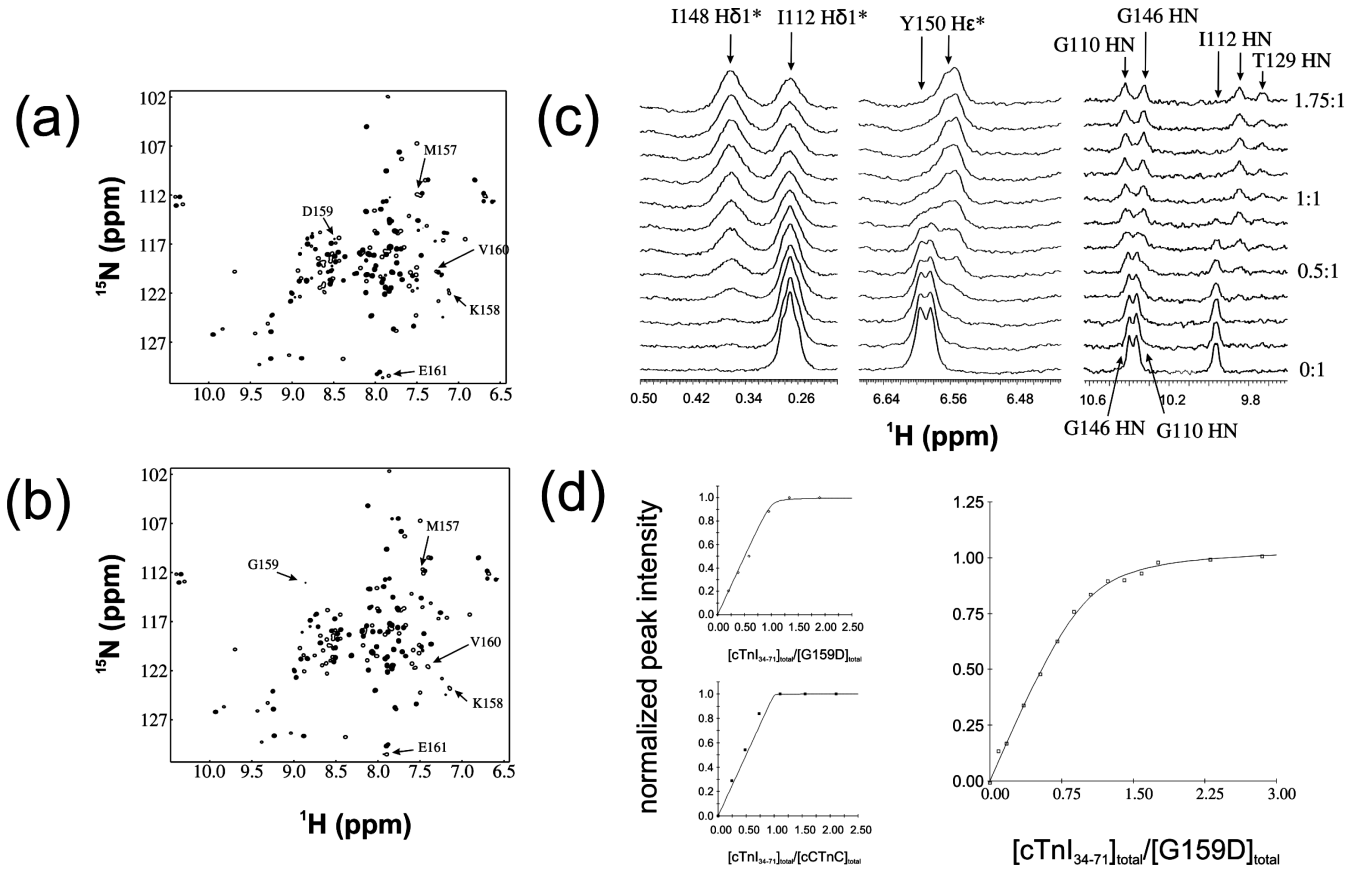

FIGURE 1: Titration of (a) G159D and (b) cCTnC with cTnI$_{34-71}$ using 2D ^{1}H−^{15}N HSQC NMR spectroscopy. The NMR samples contained 0.57 mM cCTnC and 0.56 mM G159D. Filled cross-peaks correspond to uncomplexed cCTnC or G159D, and empty cross-peaks correspond to the complex of cCTnC or G159D with cTnI$_{34-71}$. Annotated residues have the largest ^{15}N chemical shift differences and are adjacent to the mutation site. (c) 1D ^{1}H NMR stacked spectra acquired during the titration of G159D with cTnI$_{34-71}$. The concentration of G159D was reduced to 42 μM to more accurately determine the dissociation constant of cTnI$_{34-71}$ for G159D. ^{1}H resonances are labeled for residues that were isolated in the 1D spectra and used to determine the K_D. The ratios of G159D to cTnI$_{34-71}$ for a few key points in the titration are given on the right side of the spectra. The titration was continued until a cTnI$_{34-71}$:G159D ratio of ~3:1 was reached; however, the stacked 1D plots are shown up to a ratio of 1.75:1 since the peak intensities remained mostly unchanged at higher ratios. Binding curves (d) corresponding to the titration of G159D (○) and cCTnC (■) with cTnI$_{34-71}$ as monitored by 2D ^{1}H−^{15}N HSQC NMR spectroscopy are provided in the smaller plots at the left. The large plot on the right reflects the changes in signal intensity during the titration of 42 μM G159D with cTnI$_{34-71}$ (□). The binding data were averaged and normalized and then fit using the program xcrvfit (see Experimental Procedures for details).

RESULTS

cTnI$_{34-71}$ Titrations of cCTnC and G159D. In a 2D ^{1}H−^{15}N HSQC NMR spectrum, cross-peaks correlate the ^{15}N and ^{1}H chemical shifts of backbone amide NH groups. Chemical shifts are exceptionally sensitive to changes in the structure and dynamics of a protein. 2D ^{1}H−^{15}N HSQC spectra obtained for G159D (Figure 1a) and cCTnC (Figure 1b), with and without their binding partner, cTnI$_{34-71}$, demonstrate the difference in the positions of several ^{1}H−^{15}N HSQC cross-peaks, corresponding to the residues adjacent to the site of mutation. The rest of the amide chemical shifts, and the changes they undergo during the titration with cTnI$_{34-71}$, are similar, suggesting a resemblance in the overall structural folds for G159D and cCTnC, in agreement with the structure determined here (see below). The kinetics of the binding of cTnI$_{34-71}$ to G159D (Figure 1a) and cCTnC (Figure 1b) are on the NMR slow exchange time scale, in which the intensities of cross-peaks for complexed and uncomplexed species vary depending on the degree of binding. Binding curves were obtained by measuring the intensity decrease for several representative cross-peaks corresponding to the unliganded protein, which were averaged and fit to a single-binding site model (Figure 1d). K_D values were found to be 6 ± 3 μM in the case of G159D and <1 μM in the case of cCTnC. The later is in agreement with literature data (*36*).

To more accurately determine the dissociation constant of cTnI$_{34-71}$ with G159D, the titration was repeated at a concentration of G159D equal to 42 μM, which was too low for an adequate acquisition of 2D ^{1}H−^{15}N HSQC NMR spectra at each titration point (in a realistic time frame). However, there were several peaks isolated in the 1D ^{1}H NMR spectrum of G159D, which could be monitored throughout the titration (Figure 1c). Intensities at each titration point were measured for the isolated peaks, averaged, normalized, and plotted against the ratio of total cTnI$_{34-71}$ to total G159D (Figure 1d). The dissociation constant was determined to be 3.0 ± 0.6 μM, which is within experimental error of that determined at the higher concentration.

^{15}N Backbone Relaxation Data. ^{15}N backbone NMR relaxation parameters, T_1, T_2, and NOE, are the complex functions of the protein motions, including the tumbling of a protein as a whole, the motions of its independent parts, and the chemical exchange processes. Per residue T_1, T_2, and

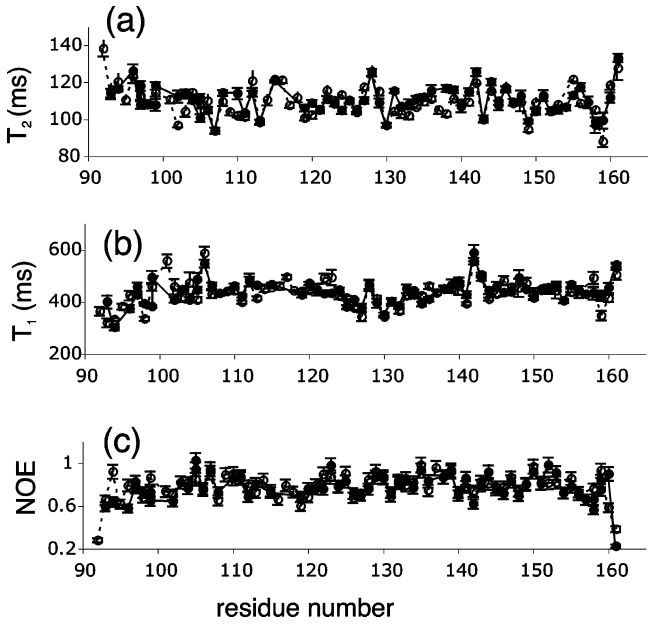

FIGURE 2: Per residue NMR relaxation parameters T_2 (a), T_1 (b), and NOE (c) for G159D (●) and cCTnC (○) in complexes with $cTnI_{34-71}$.

NOE values were determined for G159D and cCTnC alone, and in complex with $cTnI_{34-71}$ (Figure 2). T_1, T_2, and NOE values for cCTnC·$cTnI_{34-71}$ and G159D·$cTnI_{34-71}$ complexes were virtually identical within the errors of the experiments (Figure 2), implying that the presence of the mutation did not affect the dynamic properties, or the conformational flexibility, of the complex. Importantly, ^{15}N backbone T_1, T_2, and NOE values for cCTnC·$cTnI_{34-71}$ and G159D·$cTnI_{34-71}$ complexes were also similar in the area adjacent to the mutation site. Relaxation data for cCTnC were in agreement with qualitative data published previously (*37, 38*).

T_1, T_2, and NOE are per residue parameters, whereas the overall correlation time, τ_m, calculated from T_1, T_2, and NOE (Table 1), is the function of the hydrated radius of the entire protein, r_h, and consequently its molecular mass. According to the Stokes−Einstein−Debye theory (*39*)

$$\tau_m = \frac{4}{3}\pi\eta r_h^3/k_B T$$

where η is the solvent viscosity, k_B is the Boltzmann constant, and T is the temperature. As a rule of thumb, τ_m (nanoseconds) is approximated as half of the molecular mass of a protein (kilodaltons), provided that the protein tumbling is mostly isotropic. This can serve as a good estimate of the molecular mass of a protein or its complexes (*18*). An increase in τ_m, as compared to the calculated molecular mass, can result from issues such as dimerization (*40*), which is the case for skeletal protein sCTnC (*41*). We have determined τ_m values for G159D and cCTnC alone, and in complex with $cTnI_{34-71}$ (Table 1). For cCTnC and G159D, τ_m values are comparable to each other and smaller than the rule of thumb estimate, which could be explained by a lower level of bound water, for example (*42, 43*). The values of τ_m determined for G159D·$cTnI_{34-71}$ and cCTnC·$cTnI_{34-71}$ complexes were comparable to each other and to the theoretical estimate, which suggests the formation of 1:1 complexes in both cases, and the absence of dimerization and significant conformational exchange.

Differences in the Chemical Shifts of cCTnC and G159D in Complexes with $cTnI_{34-71}$. Chemical shift changes are uniquely indicative of changes in chemical environment of nuclei and, hence, in protein structure and dynamics. We have calculated the chemical shift changes of ^{15}N, ^{13}C, and ^{1}H for G159D and cCTnC in complexes with $cTnI_{34-71}$ (Figures 3 and 4). Backbone amide ^{15}N chemical shifts underwent the most significant perturbations at the end of the H-helix near the mutation site (Figures 3a and 4a). ^{15}N chemical shifts in the region where the H-helix is contacting the E-helix (residues 93−97) are also affected by the presence of the mutation but to a much lesser extent. As demonstrated by ^{15}N chemical shift changes, the overall fold of G159D and cCTnC remains similar, with the only significant perturbation being near the mutation site. Changes in ^{1}H and ^{13}C chemical shifts, especially those for the side chains, are sensitive not only to the changes in the overall fold but also to the changes in the configurational patterns, e.g., the number, energetics, and geometry of connections that stabilize the protein core or protein complex. As demonstrated by ^{13}C chemical shift changes (Figures 3b and 4b), the major perturbations occurred at several hydrophobic residues (for example, Leu^{100}, Met^{120}, Leu^{121}, and Ile^{128}) known to be responsible for the interaction with $cTnI_{34-71}$ (*17*). ^{1}H atoms, directly responsible for the majority of van der Waals and hydrophobic contacts in proteins, are the most sensitive indicators of changes in protein core and binding interfaces. As demonstrated by ^{1}H chemical shift differences (Figures 3c and 4c), significant changes occurred with the residues forming the interface between cCTnC and $cTnI_{34-71}$ (for example, Leu^{100}, Met^{103}, Met^{120}, Leu^{121}, Ile^{128}, and Leu^{136}), implying that the binding of $cTnI_{34-71}$ to cCTnC is perturbed in the presence of the mutation (*17*). Interestingly, the chemical shifts of two interior residues, Ile^{148} and Ile^{112}, which form the hydrophobic core of cCTnC, have also undergone perturbations.

Differences in the NOE Connectivities of cCTnC and G159D in Complexes with $cTnI_{34-71}$. NOE connectivites obtained from 3D ^{13}C NOESY HSQC and ^{15}N NOESY HSQC NMR spectra are typically used as distance restraints during structure calculations. It is often informative therefore to make pairwise comparisons of NOE patterns. The NOE, however, is less sensitive to long-range perturbations than the chemical shift since the intensity of NOE decreases rapidly with the distance between two nuclei: NOE $\propto 1/r^6$ (*44*). We have compared strips from 3D ^{13}C NOESY HSQC and ^{15}N NOESY HSQC NMR spectra for G159D and cCTnC for residues with significant chemical shift changes. Spectra were acquired using identical parameters, such as mixing time, which is crucial for such a comparison. The vast majority of contacts in the cCTnC spectra were accurately reproduced in the G159D spectra; however, there were some differences (Figure 5). For example, in the ^{13}C NOESY HSQC spectrum, the γ-proton of Met^{103} has more contacts in cCTnC compared to G159D, with some of these contacts being tentatively assigned to the peptide resonances (Figure 5a). The γ-proton of Ile^{112} contacted the α-proton of Asp^{149} in G159D, and the α-proton of Asp^{105} and the δ-proton of Tyr^{150} in cCTnC (Figure 5b). The α-proton of Gly^{140} contacted the γ-proton of Glu^{152} in cCTnC but not in G159D (Figure 5c). The γ-proton of Val^{160} contacted the ε-proton of Phe^{156} in G159D but not in cCTnC (Figure 5d). In the

Table 3: NMR Experiments Conducted for Structure Calculations and Chemical Shift Assignments

	nuclei	^{1}H	*x*-pts	*y*-pts	*z*-pts	*x*-sw	*y*-sw	*z*-sw	mix (ms)
^{15}N HSQC	^{1}H, ^{15}N	500	1074	192		8384.9		2026.3	−
HCCH-TOCSY	^{1}H, ^{13}C, ^{1}H	500	1024	128	104	8384.9	5998.5	10057.8	−
CBCA(CO)NNH	^{1}H, ^{13}C, ^{15}N	500	1024	118	64	8384.9	10057.2	2026.3	−
HNCACB	^{1}H, ^{13}C, ^{15}N	500	1024	118	64	8384.9	10057.2	2026.3	−
HCCONH	^{1}H, ^{13}C, ^{15}N	600	1024	160	64	8398.1	5998.5	2431.6	−
CCONH	^{1}H, ^{13}C, ^{15}N	600	1024	184	64	8398.1	12067.2	2431.6	−
^{13}C NOESY HSQC	^{1}H, ^{1}H, ^{13}C	600	1024	160	80	8398.1	5998.7	6033.7	100
^{15}N NOESY HSQC	^{1}H, ^{1}H, ^{15}N	600	1024	160	80	8398.1	5998.7	2431.6	150
^{15}N TOCSY HSQC	^{1}H, ^{1}H, ^{15}N	600	1024	160	64	8398.1	5998.7	2431.6	50
HNHA	^{1}H, ^{1}H, ^{15}N	600	1024	160	64	8398.1	5998.7	2431.6	−
HNHB	^{1}H, ^{1}H, ^{15}N	500	1024	160	64	8384.9	4998.8	2026.3	−
DQF-COSY (D_2O)	^{1}H, ^{1}H	800							
NOESY (D_2O)	^{1}H, ^{1}H	800							
^{13}C- and ^{15}N-filtered TOCSY	^{1}H, ^{1}H	600	4096	512	−	8384.9	8385.7	−	60
^{13}C- and ^{15}N-filtered NOESY	^{1}H, ^{1}H	600	4096	512	−	8384.9	8385.7	−	250
^{13}C-edited, filtered NOESY	^{1}H, ^{1}H, ^{13}C	600	1024	240	64	3595.9	3595.9	3014.0	150

^{15}N NOESY HSQC NMR spectrum, the differences in NOE patterns were less significant, with the noticeable change observed in the amide proton of Ala^{108}, which had contacts with the β-protons of Lys^{106} and Asn^{107} in G159D but not in cCTnC. These results demonstrate that the residues with the large chemical shift differences (Figure 5) also had distinct NOE connectivities in ^{13}C NOESY HSQC and ^{15}N NOESY HSQC spectra.

Structures of cCTnC and G159D in Complexes with cTnI$_{34-71}$. The ensemble containing the 20 best NMR structures of 50 calculated structures was analyzed for G159D and cCTnC. All structures had a good geometry after water refinement with >92% in most favorable and >7% in additionally allowed regions of the Ramachandran plot for G159D and cCTnC (Table 2). Structures of both proteins converged with a rmsd of <1.4 Å for all atoms for residues 95−155, including loops. The overall topology and the secondary structure for G159D and cCTnC were similar to the topology and structure of cCTnC determined by X-ray crystallography [PDB entry 1J1D (*17*)] and previously by NMR [PDB entry 1FI5 (*38*)]. The rmsd for backbone atoms between cCTnC and 1J1D was 1.2 Å for all residues, and between cCTnC and 1FI5, it was 1.4 Å (Figure 6a). A similar rmsd of 1.7 Å was reported between 1FI5 and 1J1D. The G159D structure, although similar overall, overlapped with 1J1D with a rmsd of 1.7 Å for backbone atoms of all residues (Figure 6b). G159D overlapped with cCTnC with a rmsd of 1.4 Å and with 1FI5 with a rmsd of 1.3 Å (Figure 6b). The resolution of X-ray diffraction data for 1J1D was 2.6 Å (*17*), within which structures determined in this work and reported previously have similar folds.

The packing of the cCTnC core occurs between the hydrophobic residues of α-helical regions (Leu^{97}, Phe^{101}, Leu^{117}, Met^{120}, Leu^{121}, Ile^{133}, Leu^{136}, Phe^{153}, and Met^{157}) and the two residues of the β-sheet region (Ile^{112} and Ile^{148}). The orientation of these key residues did not change in the cCTnC

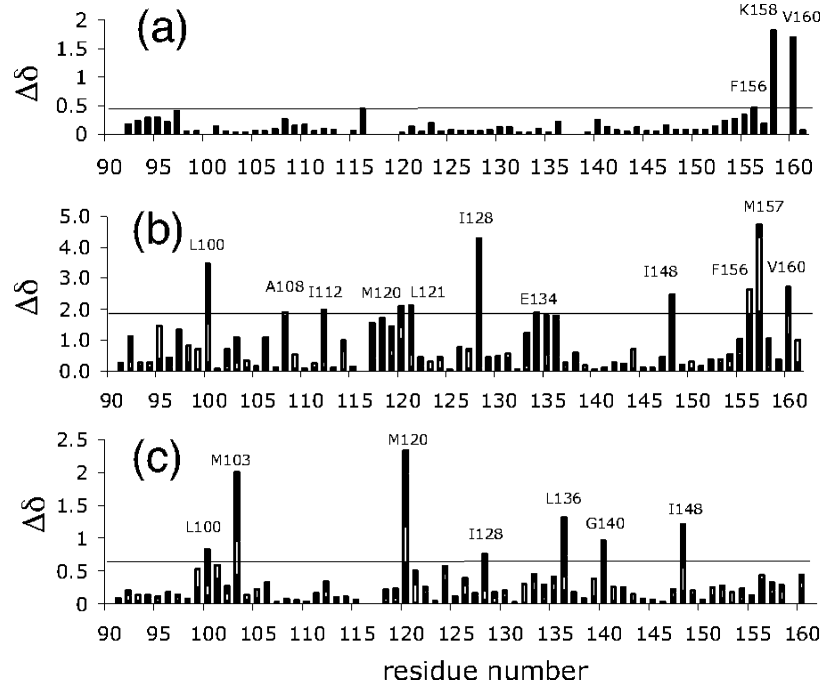

FIGURE 3: Chemical shift differences between G159D and cCTnC in complexes with cTnI$_{34-71}$ for backbone amide ^{15}N (a), side chain ^{13}C (b), and side chain ^{1}H (c) atoms. Side chain chemical shift changes for ^{13}C and ^{1}H are added together for every residue, with those of Cα and Hα colored black, those of Cβ and Hβ white, those of Cδ and Hδ red, those of Cε and H dark blue, and those of Cδ and Hδ green. Horizontal lines correspond to the average value plus one standard deviation.

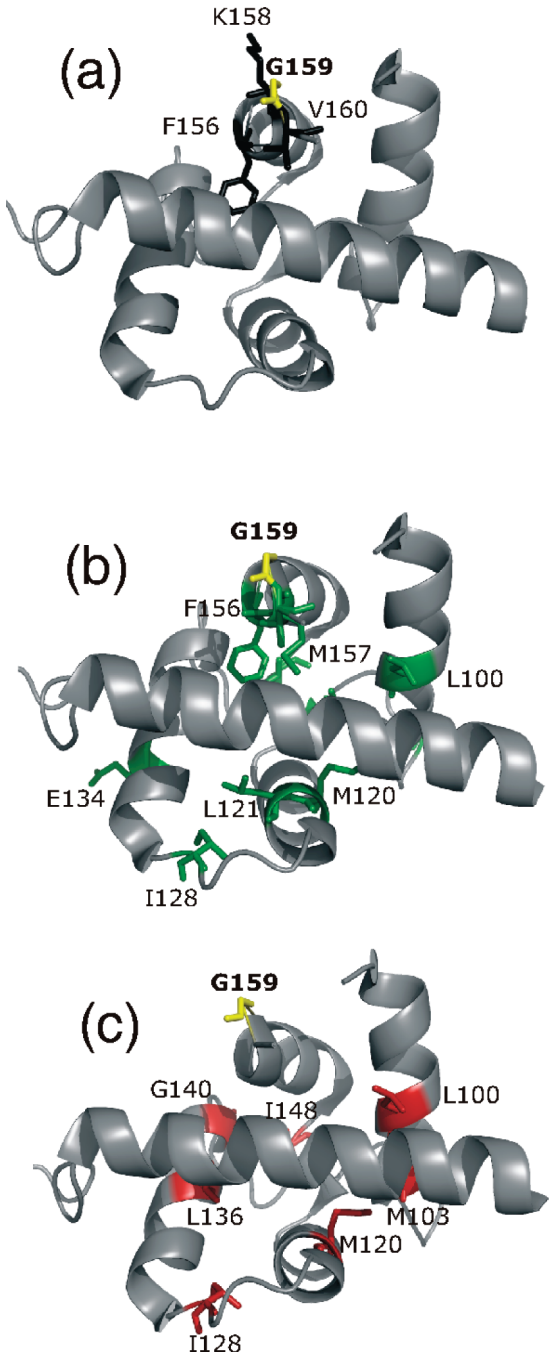

FIGURE 4: Residues with chemical shift changes visualized on the structure of cCTnC determined by X-ray crystallography (PDB entry 1J1D). Residues with significant ^{15}N chemical shift changes are colored black (a). Residues with significant side chain ^{13}C chemical shift changes are colored green (b). Residues with significant side chain ^{1}H chemical shift changes are colored red (c). Gly^{159} is colored yellow in all three panels.

and G159D structures calculated in this work as compared to 1J1D and 1FI5. Several residues such as Phe^{104} and Phe^{156} in cCTnC and G159D lack the restraints with the peptide, and thus, their positions are more flexible but are in the good agreement with the NMR structure, 1FI5. The packing interactions between helices and the protein cores of cCTnC have not been affected by the presence of G159D as demonstrated by the resultant structures. In spite of some differences in NOE contacts for Ile^{112} and Ile^{148}, the calculated structures were similar within the limits of the method. This demonstrates that among the restraints used (Table 2), many were identical, which determined the similarity between the structures.

Differences in the NOE Connectivities between cCTnC (and G159D) and $cTnI_{34-71}$ in ^{13}C-Edited, Filtered NOESY Spectra. The NOE connectivities between ^{15}N- and ^{13}C-labeled cCTnC and the unlabeled peptide $cTnI_{34-71}$ were obtained using the ^{13}C-edited, filtered NOESY pulse sequence (*45*) optimized in our laboratory for this particular complex (*46*). In this experiment, each cross-peak corresponds to a ^{1}H protein resonance on the vertical axis and to a ^{1}H peptide resonance on the horizontal axis. The ^{13}C resonance in the third dimension connects to the corresponding ^{1}H resonances on the protein, which allows for the assignment. Peptide ^{1}H assignments can be typically obtained with 2D ^{15}N- and ^{13}C-filtered TOCSY and 2D ^{15}N- and ^{13}C-filtered NOESY (*47*−*49*); however, in our case, few resonances can be unambiguously assigned due to the poor dispersion of peptide chemical shifts, which precluded the structure calculation for the entire complex. Like previous NMR studies (*38, 41, 50*), determination of the structure of the entire complex was difficult to achieve without the additional restraints between a protein and a peptide, which might be found in crystal structures but are not always desirable due to the possibility of the introduction of artifacts. The peptide in complex is predominantly α-helical, which is supported by the values of peptide chemical shifts in 2D ^{15}N- and ^{13}C-filtered TOCSY and 2D ^{15}N- and ^{13}C-filtered NOESY and their poor dispersion. The superposition of ^{13}C-edited, filtered NOESY spectra for G159D and cCTnC in complexes with $cTnI_{34-71}$ shows a similarity between contacts formed (Figure 7). Some contacts are virtually identical, for example, the contacts between Ala^{57} of $cTnI_{34-71}$ and Leu^{100} and Met^{120} of cCTnC and G159D (Figure 7a) or the contact between Leu^{62} of $cTnI_{34-71}$ and Met^{103} of cCTnC and G159D (Figure 7c). Some contacts were slightly changed, for example, the contacts between Ile^{56} of $cTnI_{34-71}$ and Thr^{124} of cCTnC and G159D (Figure 7c). One contact, between Leu^{54} of $cTnI_{34-71}$ and Val^{160} of cCTnC, was clearly missing in G159D (Figure 7b). No contacts were observed in the spectrum of G159D that were missing in the case of cCTnC. Also, the intensities of existing connectivities were not stronger in the case of G159D. This demonstrates that G159D interacts with $cTnI_{34-71}$ in a manner similar to that of cCTnC, without making new connections between the protein and the peptide and with the existing connections not being qualitatively stronger.

DISCUSSION

The task of defining the impact of mutations on the structure and function of the sarcomeric proteins and the resultant physiological behavior of the sacromere represents a substantial challenge, especially for nonlethal human mutations where the effect on the protein has to be mild to allow an individual to survive even in disease. Structural approaches, including the determination of structure using NMR or crystallography, might not provide conclusive answers when the differences in structures of mutant and wild-type proteins are not sufficiently significant to be resolved within the resolution of the chosen technique. Often, the affinities of mutated and wild-type proteins for their targets and/or ligands are unchanged. It remains unknown,

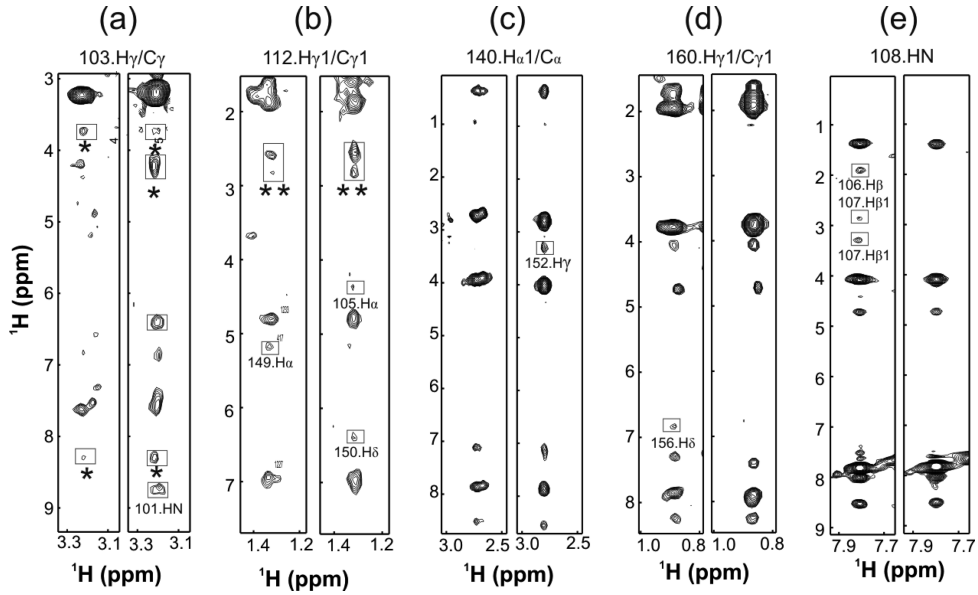

FIGURE 5: NOE strips for G159D (left) and cCTnC (right) in complexes with $cTnI_{34-71}$ obtained from 3D ^{13}C NOESY HSQC NMR spectra (a−d) and ^{15}N NOESY HSQC NMR spectra (e), where single asterisks denote the resonances tentatively assigned to the peptide and double asterisks denote resonances tentatively assigned to the protein. Assignments are indicated below each pair of plots.

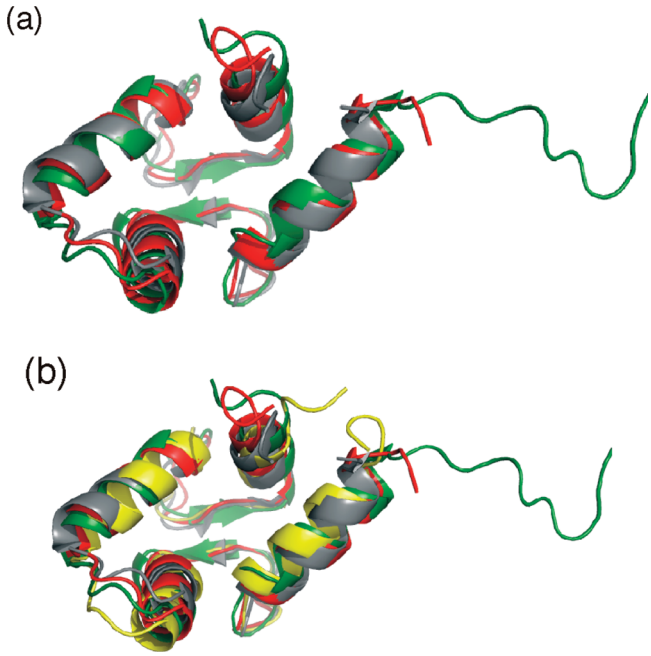

FIGURE 6: Secondary structures of cCTnC (a) and G159D (b) in complexes with the anchoring region of cTnI in comparison with previously determined structures 1J1D (gray) and 1FI5 (green). The structure of cCTnC determined in this work is colored red in both panels, and the structure of G159D is colored yellow.

therefore, whether the mutant phenotype has been caused by the changes that cannot be detected within the limits of methods. However, the necessity to study individual human mutations is evident in the growing interest in genetically tailored nutrition and medicine and, in general, will be beneficial to our understanding of current biochemical models, in our example, cardiac muscle contraction.

We have attempted to dissect the effect of the G159D mutation on the structure, dynamics, and interactions of troponin C using solution state NMR. This technique not only allows the determination of the structure but also provides a wealth of information pertaining to the chemical environment and dynamics of individual residues. Since the effects are expected to be subtle, all NMR experiments were conducted as direct side-by-side comparisons of the wild-type and G159D mutant proteins. We have found that the secondary structure, tertiary structure, and packing of the protein core have not changed for G159D in complex with $cTnI_{34-71}$ in comparison to those of the cCTnC·$cTnI_{34-71}$ complex. The dynamic behavior of G159D is also unchanged, even in the vicinity of the mutation. However, the affinity of G159D for $cTnI_{34-71}$ is reduced, and the NMR chemical shifts of protein residues in the complex are perturbed. The K_D of G159D toward $cTnI_{34-71}$ has been increased to 3 μM. The K_D of $cTnI_{34-71}$ for wild-type cCTnC is <1 μM (*36, 51*). Furthermore, the analogous region of skeletal TnI ($sTnI_{1-40}$) has been shown to bind the C-domain of skeletal TnC with a K_D of ~50 nM (*52*). Both results are significantly tighter than that established here for G159D. The differences in NMR chemical shifts were well beyond the resolution in the ^1H dimension (0.03 ppm), ^{13}C dimension (0.3 ppm), and ^{15}N dimension (0.2 ppm) in our experiments, with the most significant changes observed for residues directly involved in binding to $cTnI_{34-71}$. We have also observed the changes in NOE connectivities between the protein and the peptide, with some connectivities changed or missing. All of this evidence indicates the weakened binding and perturbed interaction between G159D and the anchoring region of cTnI ($cTnI_{34-71}$). The structure and dynamics of the protein core remain the same, however, in agreement with the G159D mutation being located at the very end of the H-helix, away from the protein core.

The binding of cCTnC to $cTnI_{34-71}$ is a key function of the C-domain. In skeletal TnC, the binding of the inhibitory region of sTnI is dependent upon the presence of the anchoring region of sTnI, with the anchoring region modulating the binding of the inhibitory region (*52*−*54*) which directly influences contractility. In insect flight muscle, the regulation of contraction is achieved entirely through the C-domain of TnC without the involvement of the N-domain and binding of the region analogous to the switch region of cTnI (*55*). The C-domain of cTnC has also been proposed

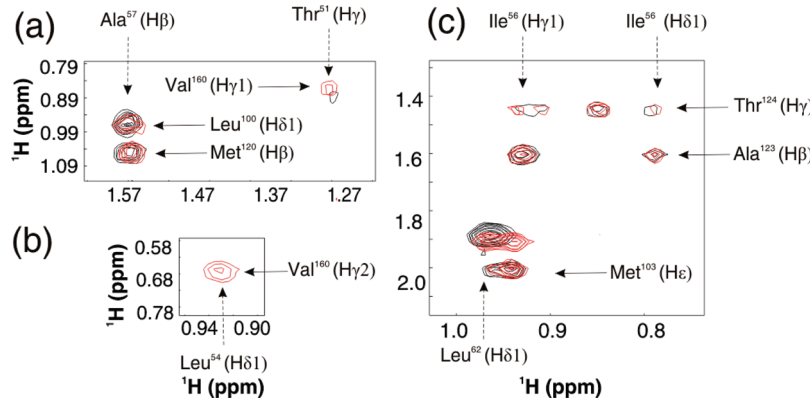

FIGURE 7: Overlap of the regions of 2D projections of the 3D ^{13}C-filtered, edited NOESY spectra, showing direct contacts between G159D (black contours) and cCTnC (red contours) with $cTnI_{34-71}$. The resonances of proteins are denoted with the horizontal solid arrows, and the resonances for the peptide are denoted with the vertical dashed arrows. The contact for G159D in panel b is missing.

to be the target of the regulatory molecule, EMD 57033, which binds exclusively to the C-domain of cTnC (*56*−*58*) and modulates the affinity of cCTnC for $cTnI_{34-71}$ (*59*). Thus, our data support the interpretation that the G159D mutation leads to impaired contractility and disease through an impaired anchoring of cTnC to the thin filament. The weaker binding to $cTnI_{34-71}$ might lead to a weaker anchoring of troponin C to the thin filament, a lower k_{on} for the switch region of cTnI (approximately residues 147−163) due to the decrease in the proximity effect, and a more pronounced inhibition of the acto-myosin ATPase. This is in agreement with slower activation kinetics in rabbit psoas fibers (*15*), which might be a more important parameter than the steady state force development (*60, 61*). Our conclusions are also in agreement with the decrease in the actin−tropomyosin activated ATPase rate and the decrease in sliding velocity (*16*).

A second possibility is that impaired function is caused by perturbations of other important long-range electrostatic interactions within the troponin complex. Electrostatic potential drops off as a function of 1/*r*, where *r* is the distance from the charge, so that it can be active 10−20 Å from the site of mutation. In the crystal structure (*17*), the N-domain of cTnC is folded over the C-domain of cTnC (Figure 8), so that Gly159 is in reasonable proximity to the binding site for the switch region of cTnI (approximately residues 147−163) (*62*), to the binding site of the inhibitory region of cTnI (approximately residues 128−147), and to the possible binding site for the cardiac specific N-terminus of cTnI (approximately residues 1−29) (*63, 64*). The binding of the N-terminus and that of the inhibitory region of cTnI are suspected to be electrostatically driven (*18, 19*), as well as influenced by phosphorylation (*65*), and the change in electrostatic potential of cCTnC might affect these interactions. A perturbed interaction of G159D with the N-terminus of cTnI has been reported (*11, 14*), which resulted in blunting the effect of PKA phosphorylation. Interestingly, the L29Q mutation has also blunted the effect of PKA phosphorylation (*10, 11, 13*) but led to hypertrophy instead (*3*). The physical parameter crucial for the development of hyper- versus hypocontractility may be the resultant affinity for the switch region of cTnI (approximately residues 147−163) (*13*) and the kinetics of this binding interaction (*11*). Another possibility to consider is that the clustering of negatively charged residues Asp^3, Asp^{87}, and Asp^{159} might produce a

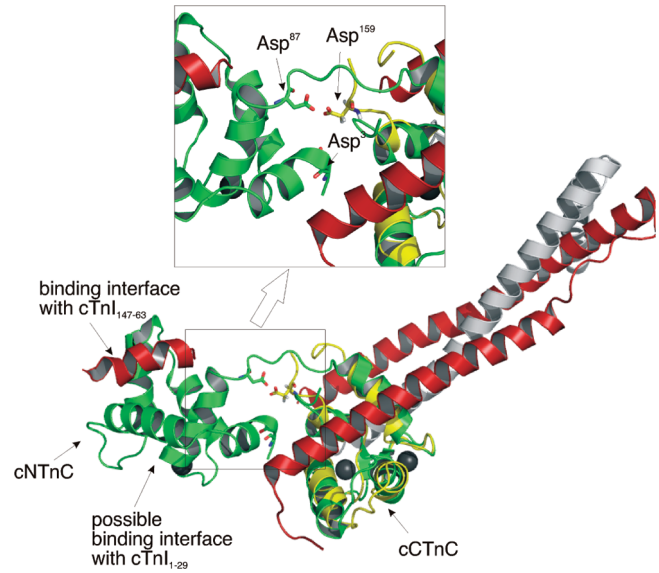

FIGURE 8: X-ray structure of the troponin complex (1JID) overlaid with G159D to demonstrate the proximity of Asp^{159} to cNTnC. Ribbon diagram of cTnC (green), cTnI (red), cTnT (gray), and G159D (yellow). The cNTnC binding site for $cTnI_{147-163}$ and the possible cNTnC binding site for $cTnI_{1-29}$ are indicated. Electrostatic residues of cNTnC in the proximity of Asp^{159} are shown as sticks (Asp^{87} and Asp^3).

cation binding site. The binding of a cation to this site could modify the interaction of troponin C with troponin I, or perhaps the flexibility of the D−E linker, either of which could impair contraction efficiency. In this work, we have determined that G159D binds to $cTnI_{34-71}$ with a weaker affinity, supported by structural data, such as changes in chemical shifts and NOE connectivities. This weakened interaction is likely to modulate the anchoring of troponin C, with a resulting increase in the level of acto-myosin inhibition. Other possibilities such as perturbed binding of the N-terminus of cTnI (approximately residues 1−29) to cNTnC through the long-range electrostatic interactions or binding of the inhibitory region of cTnI cannot be excluded (approximately residues 128−147).

ACKNOWLEDGMENT

We acknowledge NANUC, Jeff DeVries, and Nicolas Shaw for maintaining spectrometers, Angela Thiessen and David Corson for protein purification, and Olivier Julien and Monica Li for general discussions.

REFERENCES

1. Redwood, C. S., Moolman-Smook, J. C., and Watkins, H. (1999) Properties of mutant contractile proteins that cause hypertrophic cardiomyopathy. *Cardiovasc. Res. 44*, 20–36.
2. Seidman, J. G., and Seidman, C. (2001) The genetic basis for cardiomyopathy: From mutation identification to mechanistic paradigms. *Cell 104*, 557–567.
3. Hoffmann, B., Schmidt-Traub, H., Perrot, A., Osterziel, K. J., and Gessner, R. (2001) First mutation in cardiac troponin C, L29Q, in a patient with hypertrophic cardiomyopathy. *Hum. Mutat. 17*, 524.
4. Mogensen, J., Murphy, R. T., Shaw, T., Bahl, A., Redwood, C., Watkins, H., Burke, M., Elliott, P. M., and McKenna, W. J. (2004) Severe disease expression of cardiac troponin C and T mutations in patients with idiopathic dilated cardiomyopathy. *J. Am. Coll. Cardiol. 44*, 2033–2040.
5. Lim, C. C., Yang, H., Yang, M., Wang, C. K., Shi, J., Berg, E. A., Pimentel, D. R., Gwathmey, J. K., Hajjar, R. J., Helmes, M., Costello, C. E., Huo, S., and Liao, R. (2008) A novel mutant cardiac troponin C disrupts molecular motions critical for calcium binding affinity and cardiomyocyte contractility. *Biophys. J. 94*, 3577–3589.
6. Li, M. X., Wang, X., and Sykes, B. D. (2004) Structural based insights into the role of troponin in cardiac muscle pathophysiology. *J. Muscle Res. Cell Motil. 25*, 559–579.
7. Sykes, B. D. (2003) Pulling the calcium trigger. *Nat. Struct. Biol. 10*, 588–589.
8. Lim, C. C., Yang, H., Yang, M., Wang, C. K., Shi, J., Berg, E. A., Pimentel, D. R., Gwathmey, J. K., Hajjar, R. J., Helmes, M., Costello, C. E., Huo, S., and Liao, R. (2008) A Novel Mutant Cardiac Troponin C Disrupts Molecular Motions Critical For Calcium Binding Affinity And Cardiomyocyte Contractility. *Biophys. J.* (in press).
9. Muir, L. A., Tschirgi, M. L., Rajapakse, I., and Chandra, M. (2006) Rat Cardiac Troponin C Mutations L29Q and G159D Decrease Myofilament Calcium Sensitivity Without Affecting Cooperativity. *Biophysical Society Annual Meeting*, pp 529, Salt Lake City, UT.
10. Schmidtmann, A., Lindow, C., Villard, S., Heuser, A., Mugge, A., Gessner, R., Granier, C., and Jaquet, K. (2005) Cardiac troponin C-L29Q, related to hypertrophic cardiomyopathy, hinders the transduction of the protein kinase A dependent phosphorylation signal from cardiac troponin I to C. *FEBS J. 272*, 6087–6097.
11. Dong, W. J., Xing, J., Ouyang, Y., An, J., and Cheung, H. C. (2008) Structural kinetics of cardiac troponin C mutants linked to familial hypertrophic and dilated cardiomyopathy in troponin complexes. *J. Biol. Chem. 283*, 3424–3432.
12. Dweck, D., Gomes, A. V., and Potter, J. D. (2005) Functional effects of human cardiac troponin C mutations linked to familial and dilated cardiomyopathis. *Biophysical Society Annual Meeting*, p 317a, Long Beach, CA.
13. Baryshnikova, O. K., Li, M. X., and Sykes, B. D. (2008) Modulation of cardiac troponin C function by the cardiac-specific N-terminus of troponin I: Influence of PKA phosphorylation and involvement in cardiomyopathies. *J. Mol. Biol. 375*, 735–751.
14. Biesiadecki, B. J., Kobayashi, T., Walker, J. S., John Solaro, R., and de Tombe, P. P. (2007) The Troponin C G159D Mutation Blunts Myofilament Desensitization Induced by Troponin I Ser23/24 Phosphorylation. *Circ. Res. 100*, 1486–1493.
15. Preston, L. C., Ashley, C. C., and Redwood, C. S. L. (2007) DCM troponin C mutant Gly159Asp blunts the response to troponin phosphorylation. *Biochem. Biophys. Res. Commun. 360*, 27–32.
16. Mirza, M., Marston, S., Willott, R., Ashley, C., Mogensen, J., McKenna, W., Robinson, P., Redwood, C., and Watkins, H. (2005) Dilated cardiomyopathy mutations in three thin filament regulatory proteins result in a common functional phenotype. *J. Biol. Chem. 280*, 28498–28506.
17. Takeda, S., Yamashita, A., Maeda, K., and Maeda, Y. (2003) Structure of the core domain of human cardiac troponin in the Ca^{2+}-saturated form. *Nature 424*, 35–41.
18. Lindhout, D. A., Boyko, R. F., Corson, D. C., Li, M. X., and Sykes, B. D. (2005) The role of electrostatics in the interaction of the inhibitory region of troponin I with troponin C. *Biochemistry 44*, 14750–14759.
19. Vinogradova, M. V., Stone, D. B., Malanina, G. G., Karatzaferi, C., Cooke, R., Mendelson, R. A., and Fletterick, R. J. (2005) Ca^{2+}-regulated structural changes in troponin. *Proc. Natl. Acad. Sci. U.S.A. 102*, 5038–5043.
20. Blumenschein, T. M., Tripet, B. P., Hodges, R. S., and Sykes, B. D. (2001) Mapping the interacting regions between troponins T and C. Binding of TnT and TnI peptides to TnC and NMR mapping of the TnT-binding site on TnC. *J. Biol. Chem. 276*, 36606–36612.
21. Pearlstone, J. R., Chandra, M., Sorenson, M. M., and Smillie, L. B. (2000) Biological function and site II Ca^{2+}-induced opening of the regulatory domain of skeletal troponin C are impaired by invariant site I or II Glu mutations. *J. Biol. Chem. 275*, 35106–35115.
22. Li, M. X., Corson, D. C., and Sykes, B. D. (2002) Structure determination by NMR. Isotope labeling. *Methods Mol. Biol. 173*, 255–265.
23. Tripet, B., Van Eyk, J. E., and Hodges, R. S. (1997) Mapping of a second actin-tropomyosin and a second troponin C binding site within the C terminus of troponin I, and their importance in the Ca^{2+}-dependent regulation of muscle contraction. *J. Mol. Biol. 271*, 728–750.
24. Johnson, B. A., and Blevins, R. A. (1994) NMRView: A computer program for the visualization and analysis of NMR data. *J. Biomol. NMR 4*, 603–614.
25. Spyracopoulos, L. (2006) A suite of Mathematica notebooks for the analysis of protein main chain ^{15}N NMR relaxation data. *J. Biomol. NMR 36*, 215–224.
26. Lipari, G., and Szabo, A. (1982) Model-Free Approach to the Interpretation of Nuclear Magnetic-Resonance Relaxation in Macromolecules. 1. Theory and Range of Validity. *J. Am. Chem. Soc. 104*, 4546–4559.
27. Delaglio, F., Grzesiek, S., Vuister, G. W., Zhu, G., Pfeifer, J., and Bax, A. (1995) NMRPipe: A multidimensional spectral processing system based on UNIX pipes. *J. Biomol. NMR 6*, 277–293.
28. Slupsky, C. M., Boyko, R. F., Booth, V. K., and Sykes, B. D. (2003) Smartnotebook: A semi-automated approach to protein sequential NMR resonance assignments. *J. Biomol. NMR 27*, 313–321.
29. Guntert, P. (2004) Automated NMR strucutre calculation with CYANA. *Methods Mol. Biol. 278*, 353–378.
30. Jee, J., and Guntert, P. (2003) Influence of the completeness of chemical shift assignments on NMR structures obtained with automated NOE assignment. *J. Struct. Funct. Genomics 4*, 179–189.
31. Cornilescu, G., Delaglio, F., and Bax, A. (1999) Protein backbone angle restraints from searching a database for chemical shift and sequence homology. *J. Biomol. NMR 13*, 289–302.
32. Linge, J. P., Williams, M. A., Spronk, C. A., Bonvin, A. M., and Nilges, M. (2003) Refinement of protein structures in explicit solvent. *Proteins 50*, 496–506.
33. Schwieters, C. D., Kuszewski, J. J., Tjandra, N., and Clore, G. M. (2003) The Xplor-NIH NMR molecular structure determination package. *J. Magn. Reson. 160*, 65–73.
34. Laskowski, R. A., MacArthur, M. W., Moss, D. S., and Thornton, J. M. (1993) PROCHECK: A program to check the stereochemical quality of protein structures. *J. Appl. Crystallogr. 26P*, 283–291.
35. Hooft, R. W., Vriend, G., Sander, C., and Abola, E. E. (1996) Errors in protein structures. *Nature 381*, 272.
36. Li, M. X., Wang, X., Lindhout, D. A., Buscemi, N., Van Eyk, J. E., and Sykes, B. D. (2003) Phosphorylation and mutation of human cardiac troponin I deferentially destabilize the interaction of the functional regions of troponin I with troponin C. *Biochemistry 42*, 14460–14468.
37. Lindhout, D. A., and Sykes, B. D. (2003) Structure and dynamics of the C-domain of human cardiac troponin C in complex with the inhibitory region of human cardiac troponin I. *J. Biol. Chem. 278*, 27024–27034.
38. Gasmi-Seabrook, G. M., Howarth, J. W., Finley, N., Abusamhadneh, E., Gaponenko, V., Brito, R. M., Solaro, R. J., and Rosevear, P. R. (1999) Solution structures of the C-terminal domain of cardiac troponin C free and bound to the N-terminal domain of cardiac troponin I. *Biochemistry 38*, 8313–8322.
39. Bloembergen, N., Purcell, E. M., and Pound, R. V. (1948) Relaxation Effects in Nuclear Magnetic Resonance Absorption. *Phys. Rev. 73*, 679–712.
40. Baryshnikova, O. K., and Sykes, B. D. (2006) Backbone dynamics of SDF-1α determined by NMR: Interpretation in the presence of monomer-dimer equilibrium. *Protein Sci. 15*, 2568–2578.
41. Mercier, P., Spyracopoulos, L., and Sykes, B. D. (2001) Structure, dynamics, and thermodynamics of the structural domain of troponin C in complex with the regulatory peptide 1−40 of troponin I. *Biochemistry 40*, 10063–10077.
42. Cantor, C. R., and Schimmel, P. R. (1980) *Biophysical Chemistry, Part II, Techniques for the study of biological structure and function*, W. H. Freeman, New York.

43. Tanford, C. (1961) *Physical chemistry of macromolecules*, John Wiley & Sons, Inc., New York.
44. Wuthrich, K. (1986) *NMR of Proteins and Nucleic Acids*, John Wiley & Sons, Inc., New York.
45. Lee, W., Revington, M. J., Arrowsmith, C., and Kay, L. E. (1994) A pulsed field gradient isotope-filtered 3D ^{13}C HMQC-NOESY experiment for extracting intermolecular NOE contacts in molecular complexes. *FEBS Lett. 350*, 87–90.
46. Robertson, I. M., Spyracopoulos, L., and Sykes, B. D. (2007) The evaluation of isotope editing and filtering for protein-ligand interaction elucidation by NMR, *Proceedings for the International School of Biological Magnetic Resonanse, 8th Course on Biophysics and the Challenges of Emerging Threats* (Puglisi, J. D., Ed.) NATO Science Series Life and Behavioural Sciences, IOS Press, Amsterdam.
47. Gemmecker, G., Olejniczak, E. T., and Fesik, S. W. (1992) An Improved Method for Selectively Observing Protons Attached to C-12 in the Presence of H-1-C-13 spin Pairs. *J. Magn. Reson. 96*, 199–204.
48. Ikura, M., and Bax, A. (1992) Isotope-Filtered 2d NMR of a Protein Peptide Complex: Study of a Skeletal-Muscle Myosin Light Chain Kinase Fragment Bound to Calmodulin. *J. Am. Chem. Soc. 114*, 2433–2440.
49. Ogura, K., Terasawa, H., and Inagaki, F. (1996) An improved double-tuned and isotope-filtered pulse scheme based on a pulsed field gradient and a wide-band inversion shaped pulse. *J. Biomol. NMR 8*, 492–498.
50. Finley, N. L., Howarth, J. W., and Rosevear, P. R. (2004) Structure of the Mg^{2+}-loaded C-lobe of cardiac troponin C bound to the N-domain of cardiac troponin I: Comparison with the Ca^{2+}-loaded structure. *Biochemistry 43*, 11371–11379.
51. Li, M. X., Saude, E. J., Wang, X., Pearlstone, J. R., Smillie, L. B., and Sykes, B. D. (2002) Kinetic studies of calcium and cardiac troponin I peptide binding to human cardiac troponin C using NMR spectroscopy. *Eur. Biophys. J. 31*, 245–256.
52. Tripet, B., De Crescenzo, G., Grothe, S., O'Connor-McCourt, M., and Hodges, R. S. (2003) Kinetic analysis of the interactions between troponin C (TnC) and troponin I (TnI) binding peptides: Evidence for separate binding sites for the 'structural′ N-terminus and the 'regulatory′ C-terminus of TnI on TnC. *J. Mol. Recognit. 16*, 37–53.
53. Sheng, Z., Pan, B. S., Miller, T. E., and Potter, J. D. (1992) Isolation, expression, and mutation of a rabbit skeletal muscle cDNA clone for troponin I. The role of the NH2 terminus of fast skeletal muscle troponin I in its biological activity. *J. Biol. Chem. 267*, 25407–25413.
54. Potter, J. D., Sheng, Z., Pan, B. S., and Zhao, J. (1995) A direct regulatory role for troponin T and a dual role for troponin C in the Ca^{2+} regulation of muscle contraction. *J. Biol. Chem. 270*, 2557–2562.
55. De Nicola, G., Burkart, C., Qiu, F., Agianian, B., Labeit, S., Martin, S., Bullard, B., and Pastore, A. (2007) The structure of *Lethocerus* troponin C: Insights into the mechanism of stretch activation in muscles. *Structure 15*, 813–824.
56. Pan, B. S., and Johnson, R. G., Jr. (1996) Interaction of cardiotonic thiadiazinone derivatives with cardiac troponin C. *J. Biol. Chem. 271*, 817–823.
57. Kleerekoper, Q., and Putkey, J. A. (1999) Drug binding to cardiac troponin C. *J. Biol. Chem. 274*, 23932–23939.
58. Li, M. X., Spyracopoulos, L., Beier, N., Putkey, J. A., and Sykes, B. D. (2000) Interaction of cardiac troponin C with Ca^{2+} sensitizer EMD 57033 and cardiac troponin I inhibitory peptide. *Biochemistry 39*, 8782–8790.
59. Wang, X., Li, M. X., Spyracopoulos, L., Beier, N., Chandra, M., Solaro, R. J., and Sykes, B. D. (2001) Structure of the C-domain of human cardiac troponin C in complex with the Ca^{2+} sensitizing drug EMD 57033. *J. Biol. Chem. 276*, 25456–25466.
60. Cheng, H., Lederer, M. R., Lederer, W. J., and Cannell, M. B. (1996) Calcium sparks and $[Ca^{2+}]_i$ waves in cardiac myocytes. *Am. J. Physiol. 270*, C148−C159.
61. Takamatsu, T., and Wier, W. G. (1990) Calcium waves in mammalian heart: Quantification of origin, magnitude, waveform, and velocity. *FASEB J. 4*, 1519–1525.
62. Li, M. X., Spyracopoulos, L., and Sykes, B. D. (1999) Binding of cardiac troponin-I147−163 induces a structural opening in human cardiac troponin-C. *Biochemistry 38*, 8289–8298.
63. Finley, N., Abbott, M. B., Abusamhadneh, E., Gaponenko, V., Dong, W., Gasmi-Seabrook, G., Howarth, J. W., Rance, M., Solaro, R. J., Cheung, H. C., and Rosevear, P. R. (1999) NMR analysis of cardiac troponin C-troponin I complexes: Effects of phosphorylation. *FEBS Lett. 453*, 107–112.
64. Gaponenko, V., Abusamhadneh, E., Abbott, M. B., Finley, N., Gasmi-Seabrook, G., Solaro, R. J., Rance, M., and Rosevear, P. R. (1999) Effects of troponin I phosphorylation on conformational exchange in the regulatory domain of cardiac troponin C. *J. Biol. Chem. 274*, 16681–16684.
65. Keane, N. E., Quirk, P. G., Gao, Y., Patchell, V. B., Perry, S. V., and Levine, B. A. (1997) The ordered phosphorylation of cardiac troponin I by the cAMP-dependent protein kinase: Structural consequences and functional implications. *Eur. J. Biochem. 248*, 329–337.

BI801165C